Non-traffic-induced vehicle stops and their impact on traffic congestion with drone footage

Oriol Pascual-Anglès*[1], Jasso Espadaler-Clapés[1], Manos Barmpounakis[1], and Nikolas Geroliminis[1,2]

[1]Mobilysis, Lausanne, Switzerland
[2]Urban Transport Systems Laboratory, EPFL, Lausanne, Switzerland

Short summary

This study investigates the impact of non-traffic-induced vehicle stops – such as pick-up/drop-off activities, illegal parking, and delivery operations – on urban traffic congestion. We propose a novel methodology for identifying these stops using high-resolution drone data and machine learning techniques, including Random Forest and XGBoost. Stops are detected from vehicle trajectories and classified as traffic-induced or non-traffic-induced based on contextual features, such as stop duration and location characteristics. While non-traffic-induced stops are predominantly observed in the rightmost lane – as expected – the results further provide a quantitative characterization of their temporal and spatial patterns, enabling the identification of critical hotspots and the estimation of their impact on overall traffic dynamics. In addition, we find that short-duration non-traffic-induced stops increase lane-changing activity, circulating vehicles change lanes to avoid the stopped vehicle, which can lead to shockwave formation and reduced traffic flow efficiency.
Keywords: Traffic congestion; vehicle stops; traffic, network, and mobility management; drone data.

1 Introduction

Vehicle stops in urban areas exhibit a dual nature. Traffic-induced stops—caused by congestion, traffic signals, or queue formation—are inherently linked to traffic system dynamics. In contrast, non-traffic-induced stops—such as passenger pick-up/drop-off, illegal parking, or delivery activities—occur independently of traffic conditions yet can significantly disrupt traffic patterns. These stops may lead to increased travel times, lane blockages, reduced road capacity, and safety risks (Boyac & Geroliminis, 2011; Cao et al., 2016; Espadaler-Clapés et al., 2023). Several studies have highlighted the impact of delivery-related illegal parking on traffic congestion and emissions. (Alho et al., 2018) found that optimized dedicated delivery bays reduce freight vehicle double-parking and associated congestion, increasing average speeds. Similarly, (Iwan et al., 2018) demonstrates speed increases and emission reductions when delivery vehicles use designated areas instead of double-parking. A simulation study by (Kladeftiras & Antoniou, 2013) extends these findings to all vehicle stops, showing that eliminating double-parking can increase speeds by 44% and reduce travel time by 47%. Additionally, (Barmpounakis & Geroliminis, 2020) realized the potential of drone data for analyzing service-related stop impacts on traffic, while (Loder et al., 2022) explored the use of drone data for monitoring freight vehicle stopping behavior. Despite attention to delivery-related stops and double-parking, the broader phenomenon of non-traffic-induced stops remains underexplored, primarily due to the lack of detection tools. Short-duration stops are particularly challenging to detect and quantify, as they are transient events whose impacts may not be captured by conventional monitoring systems. Consequently, detecting non-traffic-induced stops and assessing their congestion impacts is essential for developing effective traffic management strategies.

In this paper, we propose a novel methodology for the identification and classification of non-traffic-induced stops using high-resolution vehicle trajectories extracted from drone data and machine learning techniques. The proposed approach is trained and applied to a real-world dataset collected in Athens, Greece. Subsequently, we investigate the impact of such stops on traffic conditions and driver behavior, with a particular focus on lane usage and short-duration stops.

2 Methodology

Data description

A large-scale data collection campaign was conducted in Athens, Greece, from the 20th to the 24th of September 2024. During this period, a swarm of eight drones was deployed to monitor traffic conditions at ten distinct locations during morning and afternoon peak hours. The locations include a mix of arterial roads, intersections, and urban streets. The drones recorded high-resolution video footage at 4K (3840x2160) and 29.97 FPS, which was then processed to extract vehicle trajectories using computer vision techniques. Further details about the data collection campaign and the processing of drone data can be found in (Barmpounakis et al., 2025). The resulting dataset contains more than a million vehicle trajectories, and 130 hours of drone footage.

A subset of the collected data was selected for the analysis of non-traffic-induced stops. This subset includes data from four locations, which were chosen based on their high frequency and variety of non-traffic-induced stops, such as bus stops, pick-up/drop-off operations, and illegal parking. The selected locations also present different traffic conditions and road topologies, which allows for the development of a robust and transferable detection algorithm and enables a more comprehensive analysis

Stop identification and classification

The stop identification and classification follow a three-step procedure. First, stops were detected from vehicle trajectories through speed thresholds and temporal filtering. Then, each detected stop was enriched with contextual information regarding the spatial location, stop duration and surrounding traffic conditions. Finally, a machine learning classification algorithm was trained to classify stops as either traffic-induced or non-traffic-induced stops based on the extracted features.

To identify stops, trajectories were first downsampled to 1 Hz to reduce noise and computational complexity. Then, trajectories located within 5 m of the video frame border were filtered out to avoid noisy detections caused by slight positional oscillations of the drone. Next, we defined a stop as the period during which a vehicle's speed is below a threshold of 5 km/h for a minimum duration of 10 seconds. To prevent the fragmentation of a single stop into multiple detections, a temporal buffer of 2 seconds was applied between consecutive stops of the same vehicle. Following the detection, the resulting stops were enriched with multiple features, which were subsequently used for the classification of stops.

A total of 13 videos from four selected locations (see Figure 1), accounting for 42,794 vehicle trajectories, were processed and manually annotated to create a ground truth dataset. The annotation process involved visually inspecting the video footage and categorizing each stop based on its context and characteristics. The resulting ground truth dataset is composed of 884 non-traffic-induced stops (668 cars, 182 buses, and 34 trucks), and 12,485 traffic-induced stops (11,602 cars, 607 buses, and 276 trucks). An 80%-20% training-test split was performed using stratified random sampling, with the video identifier and the stop type as stratification variables. Given the strong class imbalance, class weights were computed as $w_i = \frac{N}{K \cdot n_i}$, where N is the total number of samples, K is the number of classes and n_i is the number of samples in class i. Two different classification algorithms were considered: a Random Forest model (RF) and an eXtreme Gradient Boosting (XGB) classifier. The RF hyperparameters were optimized through a grid search with 3-fold cross-validation, using the F1-score as the evaluation metric, while XGB parameters were tuned using Bayesian optimization, also with 3-fold cross-validation and F1-score as the objective function. Both models were trained separately for each vehicle type using those stops corresponding to that specific vehicle type, except for trucks for which all stops were used due to the low number of samples. Model performance was evaluated on the testing set using F1-score, precision, recall, and confusion matrices. A feature selection process was carried out using the feature importance scores from the trained models – mean impurity decrease for RF and weight for XGB – to identify the most relevant features for the classification task and reduce model complexity. The remaining features are presented in Table 2, and the models performance results are summarized in Table 1. The XGB models outperform the RF models for all vehicle types, and thus are selected for the subsequent analysis.

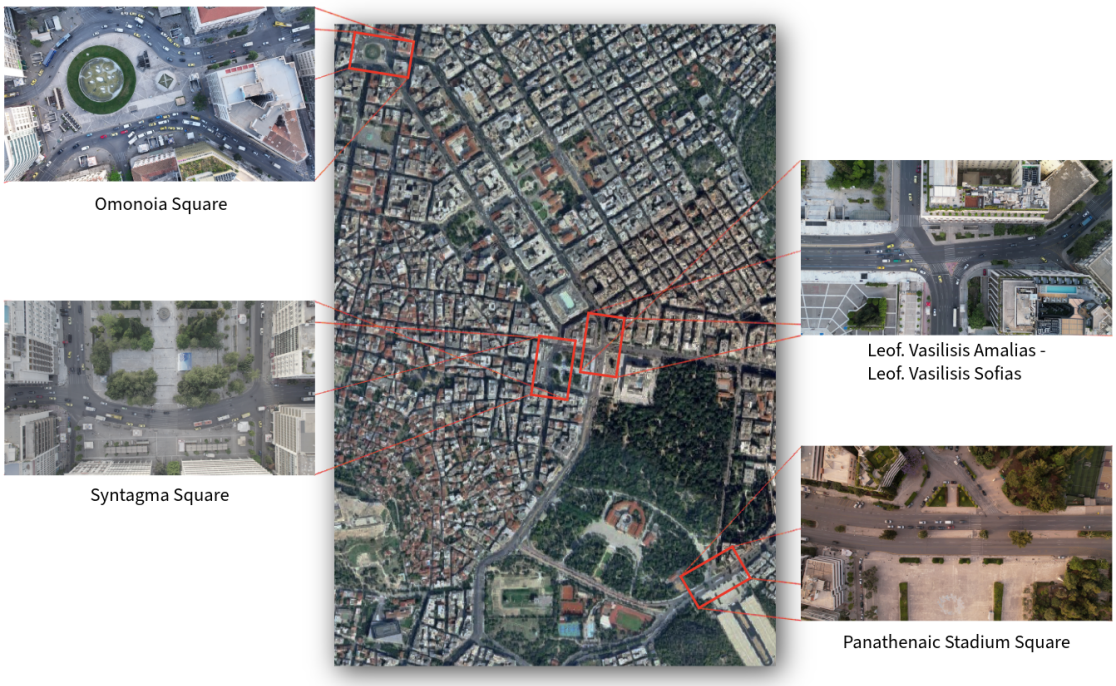


Figure 1: Selected locations for the ground truth dataset.

Table 1: Classification performance of the RF and XGB models.

Model	Vehicle type	F1-score	Precision	Recall
RF	Car	0.85	0.87	0.86
XGB	Car	0.88	0.86	0.87
RF	Bus	0.83	0.83	0.83
XGB	Bus	0.82	0.89	0.85
RF	Truck	0.82	0.91	0.86
XGB	Truck	0.84	0.91	0.87

3 Results and discussion

This section examines the impact of non-traffic-induced stops on traffic conditions. The best-performing models for each vehicle type were used to predict the type of stop at a new location, selected for its clearly defined lane structure and substantial amount of non-traffic-induced stops, which facilitates the analysis of their effects on traffic flow. The selected location corresponds to a segment of the arterial road Leof. Vasilisis Amalias with four lanes and a bus stop located on the rightmost lane in each direction. The dataset for this location comprises 6 hours and 20 minutes of drone footage, 32,376 vehicle trajectories, and 307 non-traffic-induced stops.

A spatial overview of non-traffic-induced stops is obtained using a two-variable heatmap. The study area is discretized into a grid of 50 cm x 50 cm cells, for which the average stop duration and the stop frequency per cell are computed. Vehicles are represented using rotated bounding boxes, thus expanding through several bins and resulting in a smoother heatmap and a more accurate representation of the occupied space. The resulting heatmap (Figure 2) combines contour lines representing stop frequency and a color gradient representing average stop duration. The contour lines follow a topographic representation, with one line per increment of 1 stop/hour, starting from 2 stops/hour, while the color scale ranges from green (short stops) to red (stops longer than 300 seconds).

The heatmap reveals that non-traffic-induced stops are mainly concentrated on the rightmost lanes, which provide access to the pedestrian area and bus stops. In the southbound direction,

Table 2: Stop-related features used for classification.

Type	Feature	Description
Location characteristics	Vehicle flow	Number of non-stop trajectories divided by the recording time.
	Location mean speed	Average speed of the trajectories at the stop location.
	Stop count	Number of stops at the location.
	Distance to a bus stop	Distance from the stop to the nearest bus stop (only for buses).
Surrounding conditions	Mean relative speed	Average speed to the surrounding vehicles during the stop.
	Max relative speed	Maximum speed to the surrounding vehicles during the stop.
	Simultaneous stops beginning	Number of stops beginning at the same time with a $\pm$ 5 second threshold.
	Simultaneous stops ending	Number of stops ending at the same time with a $\pm$ 5 second threshold.
	Free space in front	Percentage of free space 50 m downstream of the stop location.
	Number of vehicles in front	Number of vehicles 50 m downstream of the stop location.
	Mean speed in front	Average speed of the vehicles 50 m downstream of the stop location.
Stop characteristics	Stop duration	Duration of the stop in seconds.
	Vehicle mean speed	Average speed of the vehicle during the stop (under the 5 km/h threshold).
Trajectory characteristics	Azimuth difference before	Difference between the trajectory azimuth 5 m before and during the stop.
	Azimuth difference after	Difference between the trajectory azimuth 5 m after and during the stop.

clusters of long-duration stops are observed along the lane, with a notable concentration around the bus stop, reaching on average 6 stops per hour. In this area, stops of approximately three minutes on average are observed. This exceeds the typical duration of a bus stop, which is around 30 seconds, and most likely reflects illegal parking or extended pick-up/drop-off activities. In the opposite direction, non-traffic-induced stops appear less frequent and generally shorter in duration, although a localized cluster of long-duration stops is still observed. Overall, the heatmap demonstrates that non-traffic-induced stops are not uniformly distributed, but rather occur in the rightmost lanes, while stops elsewhere are rare and may correspond to false positives.

To further investigate and characterize stop behavior for each direction, we enriched stops with lane information by manually defining lane polygons by carefully extracting the coordinates of the lane limits. This lane assignment enables a disaggregated analysis of stop behavior per lane and, subsequently, their impact on traffic conditions. The distribution of stop duration by vehicle type for the rightmost lanes is presented in Figure 3. The boxplot corroborates the patterns observed in the heatmap: stops in the southbound direction rightmost lane are both more frequent and considerably longer than those on the opposite direction. In particular, some southbound direction rightmost lane stops last up to the full duration of a drone recording, around 18 minutes, whereas stops in the northbound direction rarely exceed 4 minutes. Moreover, 50 % of the bus stops on the southbound direction last between 2.5 and 5 minutes, indicating atypical behavior compared to standard dwell times, supporting the hypothesis of longer pick-up/drop-off activities such as those related to touristic buses or intercity buses. Car stops represent a substantial share of the stops in this direction, with lower median values (around 90 seconds) than buses but higher variability,



Figure 2: Heatmap of non-traffic-induced stops. The average length of the stop is represented by the color, while stop frequency is represented via contour lines.

reflecting a mix of short pick-up/drop-off events and longer illegal parking. In contrast, stops in the northbound rightmost lane are less frequent and generally shorter, with a few outliers associated with buses. These distributions suggest that the southbound direction is heavily affected by long and frequent non-traffic-induced stops, most likely blocking the rightmost lane for long periods of time to which traffic is progressively adapted. Conversely, the northbound direction rightmost lane experiences more sporadic stop events, which may induce sharper disruptions in traffic flow, such as sudden lane changes and speed drops. Given this distinction, the subsequent analysis focuses on the latter case, where stops are expected to cause more abrupt perturbations and shockwaves. To this end, we further filter the remaining stops by removing those with a duration longer than 150 seconds, resulting in a subset of 44 stops.

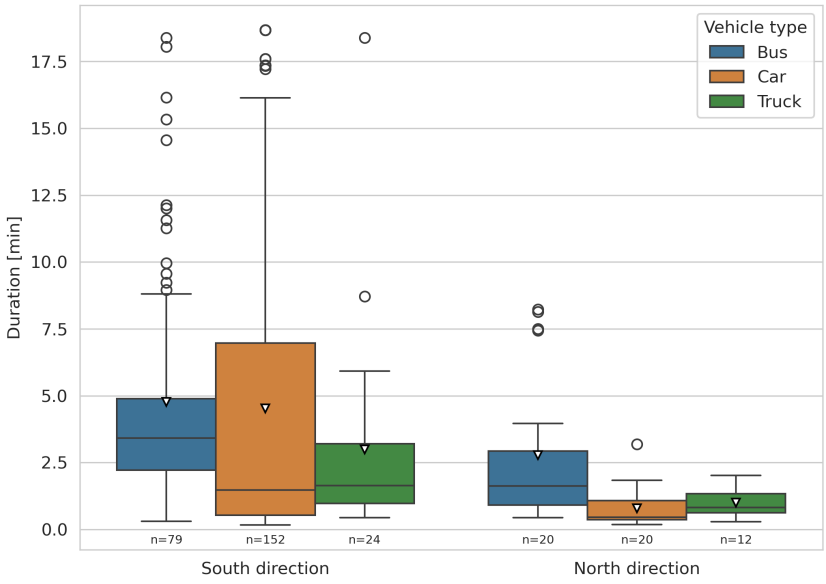
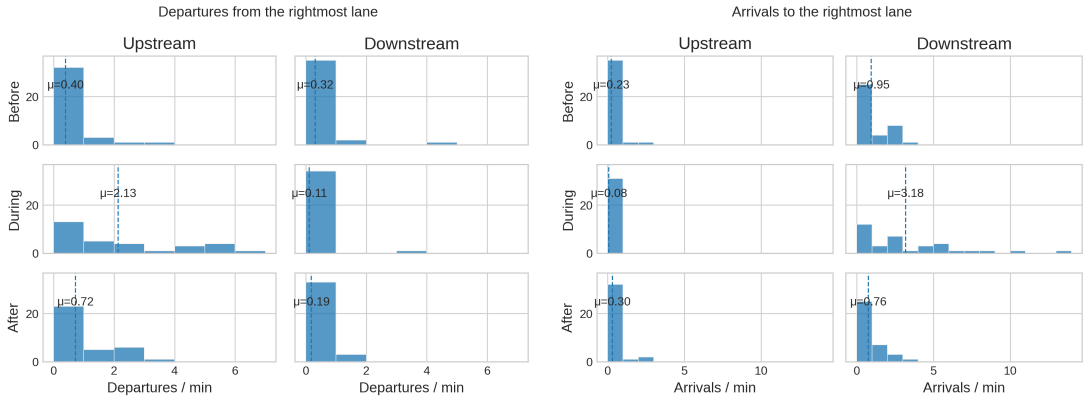


Figure 3: Distribution of stop duration by vehicle type for the rightmost lanes.

We then proceed to scrutinize the impact of the 44 non-traffic-induced stops in the northbound direction rightmost lane. The aim is to identify changes in traffic behavior caused by the stops, such as speed drops, lane changes, and shockwave formation. To do so, we analyze the trajectories of vehicles located in the vicinity of each stop, considering distinct periods before, during, and after the stop event. We define the vicinity as a 50 m lane segment both upstream and downstream of the stop location, and a temporal window of 90 seconds before and after the stop is considered to reduce variability and ensure comparability across time intervals.

For each spatio-temporal segment, we compute the number of lane changes, distinguishing between lane departures and lane arrivals. These counts are normalized by the corresponding observation time – 90 seconds for the pre- and post-stop periods, and the actual stop duration for the during-stop period – to obtain lane-change rates expressed in lane changes per minute. Given that the mean stop duration is 55 seconds, this normalization yields a representative estimate of the lane-changing intensity during the stops. The resulting lane-change rates histograms are presented in Figure 4 for the different spatio-temporal configurations. The results indicate a clear increase in lane-changing activity during stop events. In particular, upstream of the stop location, vehicles departing from the rightmost lane increase to an average of 2.13 lane-changes per minute, while downstream, lane arrivals rise to 3.18 lane changes per minute. These values are approximately five and three times higher than the corresponding pre-stop ratios for upstream departures and downstream arrivals, respectively. These findings suggest that stops create a temporary bottleneck in which vehicles are forced to change lanes to avoid the stopped vehicle, and return to the rightmost lane after overtaking the stopped vehicle.



(a) Lane departures (b) Lane arrivals

Figure 4: Lane changes per minute before, during and after the stop, and upstream and downstream of the stop location.

To visualize the above findings, we construct a four minute time-space diagram for a representative stop event. The diagram displays the trajectories of vehicles in the rightmost lane and the adjacent lane, with the non-traffic-induced stops highlighted in gray. We highlight lane-changing events with red and blue dots for lane departures and arrivals, respectively. Traffic lights locations are indicated with horizontal dashed lines, while green areas represent the green phase, which is equal for the two lights. This information enables a clear understanding of the traffic dynamics, and helps to distinguish between shockwaves arising from the stop and those caused by traffic signals. The resulting time-space diagram is presented in Figure 5. The plot clearly illustrates how differently the two green phases develop. During the first green phase, a vehicle stops in the rightmost lane, which blocks the lane circulation and causes up to seven vehicles to change lanes and join the adjacent lane. Vehicles in this lane are forced to cooperate, by intermittently yielding to the vehicles arriving. This lane-changing activity leads to lower speeds and creates small shockwaves that propagate upstream, as evidenced by the trajectories shape and speeds below 10 km/h. In contrast, during the second green phase, the stopped vehicle resumes its movement, and the vehicles in the rightmost and adjacent lanes are able to move freely at higher speeds. Even so, some lane-changing activity on the adjacent lane causes some temporal perturbations. The stop event is further illustrated in Figure 6, which shows screenshots of the stop event at different time steps: (A) a first vehicle has changed lanes to avoid the stopped vehicle while the second and third vehicles are already starting to perform the lane change maneuver (in orange), (B) and (C) show two cooperative interactions which create a shockwave in the adjacent lane and congestion appears (in blue and red), and (D) no more cooperation is observed and the adjacent lane returns to free flowing conditions while vehicles in the rightmost lane accumulate behind the stopped vehicle (in white).

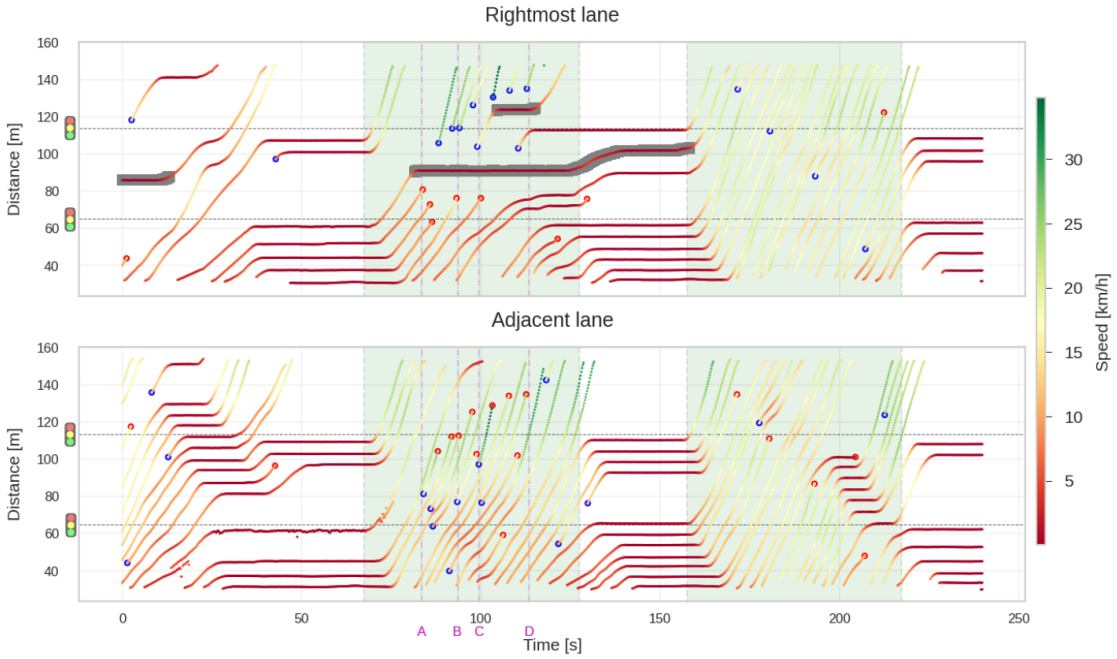


Figure 5: Two-lane time-space diagram of a non-traffic-induced stop event for the rightmost lane and adjacent lane. The detected stops are highlighted in gray, and lane departures and arrivals are represented by red and blue dots, respectively. Horizontal dashed lines indicate traffic light, while green areas represent the green phase. A, B, C and D indicate the time steps corresponding to the screenshots in Figure 6.

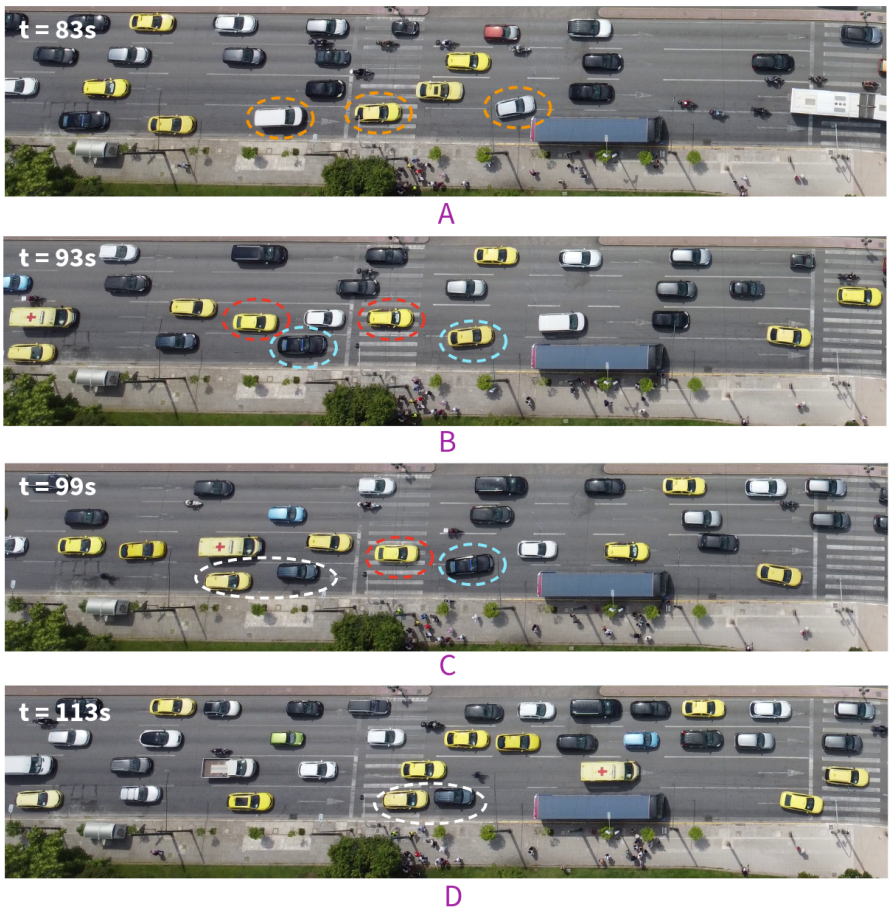


Figure 6: Screenshots corresponding to Figure 5.

4 Conclusions

The research presented in this paper introduces a new methodology for identifying non-traffic-induced vehicle stops using drone data and machine learning techniques. The methodology was trained and validated on a real-world dataset collected in Athens, Greece. The results uncover the existence of several types of non-traffic-induced stops, from short duration pick-up/drop-off events to long-term illegal parking. Furthermore, we find that short non-traffic-induced stops significantly increase lane-changing activity, which leads to the formation of shockwaves and reduces traffic flow efficiency on the rightmost and adjacent lanes. The findings emphasize the need for large-scale experiments with high-resolution data, that capture the transient nature of non-traffic-induced stops effects on traffic conditions, such as microscopic lane-changing behavior and shockwave formation and dissipation. Future research should focus on assessing the impact of non-traffic-induced stops at a macroscopic level, such as their contribution to travel time increases, and analyzing the usage of designated areas for pick-up/drop-off activities, such as bus and taxi stops, to understand the extent to which they are used for their intended purpose, and the impact of their misuse on traffic conditions.

Acknowledgements

This research was conducted as part of the ACUMEN project, which is funded by the European Union's Horizon Europe research and innovation program under grant agreement No. 101103808. This work received funding from the Swiss State Secretariat for Education, Research and Innovation (SERI).

References

Alho, A. R., de Abreu e Silva, J., de Sousa, J. P., & Blanco, E. (2018). Improving mobility by optimizing the number, location and usage of loading/unloading bays for urban freight vehicles. *Transportation Research Part D: Transport and Environment*, *61*, 3-18. (Innovative Approaches to Improve the Environmental Performance of Supply Chains and Freight Transportation Systems) doi: https://doi.org/10.1016/j.trd.2017.05.014

Barmpounakis, E., Espadaler-Clapés, J., Tsitsokas, D., Mordan, T., & Geroliminis, N. (2025). A new perspective on urban mobility through large-scale drone experiments for smarter, sustainable cities. *Drones*, *9*(9). doi: 10.3390/drones9090637

Barmpounakis, E., & Geroliminis, N. (2020). On the new era of urban traffic monitoring with massive drone data: The pneuma large-scale field experiment. *Transportation Research Part C: Emerging Technologies*, *111*, 50-71. doi: https://doi.org/10.1016/j.trc.2019.11.023

Boyac, B., & Geroliminis, N. (2011). Estimation of the network capacity for multimodal urban systems. *Procedia - Social and Behavioral Sciences*, *16*, 803-813. (6th International Symposium on Highway Capacity and Quality of Service) doi: https://doi.org/10.1016/j.sbspro.2011.04.499

Cao, Y., Yang, Z. Z., & Zuo, Z. Y. (2016). The effect of curb parking on road capacity and traffic safety. *European Transport Research Review*, *9*(1), 4. doi: 10.1007/s12544-016-0219-3

Espadaler-Clapés, J., Barmpounakis, E., & Geroliminis, N. (2023). Empirical investigation of lane usage, lane changing and lane choice phenomena in a multimodal urban arterial. *Transportation Research Part A: Policy and Practice*, *172*, 103674. doi: https://doi.org/10.1016/j.tra.2023.103674

Iwan, S., Kijewska, K., Johansen, B. G., Eidhammer, O., Małecki, K., Konicki, W., & Thompson, R. G. (2018). Analysis of the environmental impacts of unloading bays based on cellular automata simulation. *Transportation Research Part D: Transport and Environment*, *61*, 104-117. (Innovative Approaches to Improve the Environmental Performance of Supply Chains and Freight Transportation Systems) doi: https://doi.org/10.1016/j.trd.2017.03.020

Kladeftiras, M., & Antoniou, C. (2013). Simulation-based assessment of double-parking impacts on traffic and environmental conditions. *Transportation Research Record*, *2390*(1), 121-130. doi: 10.3141/2390-13

Loder, A., Otte, T., & Bogenberger, K. (2022). Using large-scale drone data to monitor and assess the behavior of freight vehicles on urban level. *Transportation Research Record*, *2676*(11), 496-507. doi: 10.1177/03611981221093620